Songklanakarin J. Sci. Technol.
40 (3), 676-681, May - Jun. 2018

http://www.sjst.psu.ac.th

Original Article

Using probabilistic neural network to analyze the binary stars Schulte 3, EY Cep, HD 101131, and Haro 1-14c

Ali Pirkhedri* and Kamal Ghaderi

Department of Science and Engineering, Marivan Branch, Islamic Azad University, Marivan, Iran

Received: 8 November 2016; Revised: 14 March 2017; Accepted: 27 March 2017

Abstract

The use of artificial neural networks (ANNs) in physical sciences has increased recently. Determining the orbital elements of binary systems helps us to obtain fundamental information. In this paper, ANNs were used to find the corresponding orbital and spectroscopic elements of four double-lined spectroscopic binary stars: Schulte 3, EY Cep, HD 101131, and Haro 1-14c. The orbital parameters of the radial velocity curve obtained from ANNs were compared with other traditional methods and we show that the proposed method is of high accuracy. Our numerical results are in good agreement with those obtained by others using nonlinear regression methods. We show the validity of our new method in a wide range of different types of binary. In this method, the time consumed is considerably less than in the other traditional methods. The present method is applicable to orbits of all eccentricities and inclination angles and enables one to vary all of the unknown parameters simultaneously.

Keywords: probabilistic neural network, binary systems, eclipsing, velocity curve

1. Introduction

Artificial neural networks (ANNs), are one of the artificial intelligence methods and have become to play an important role in our scientific or personal lives. The wide applicability of ANNs stems from their flexibility and ability to model linear and non-linear systems without prior knowledge of an empirical model. This gives ANNs an advantage over traditional fitting methods for scientific applications.

In recent years, ANNs have been widely used in astronomy for applications such as star/galaxy discrimination, galaxy morphological classification, and spectral classification of stars (Bazarghan *et al.,* 2008). Following Bazarghan *et al.* (2008), we employ probabilistic neural networks (PNNs). An example of a PNN is shown in Figure 1. This network was investigated in ample detail by Bazarghan *et al.* (2008). The method of a probabilistic neural network (PNN) is a new tool to derive orbital parameters of the spectroscopic binary stars.

*Corresponding author
Email address: pirkhedri60@gmail.com

The study of both light and radial velocity V_R curves of binary stars has the potential to provide important information, such as the masses and radii of individual stars, which has an important role in understanding the present state and evolution of many interesting stellar objects. One of the usual methods to analyze the velocity curve is the method of Lehmann-Filhés (1894). Some other methods were also introduced by Russell (1902) and Sterne (1941). The different methods for V_R curve analysis have been reviewed in ample detail by Karami and Teimoorinia (2007). They showed the validity of applying their new method to a wide range of different types of binary systems (Karami *et al.,* 2008; Karami & Mohebi, 2007a, 2007b, 2009).

Schulte 3 is a double-lined eclipsing binary and it is a probable member of the Cyg OB2 region. The spectral type is O6IV and O9III for the primary and secondary stars, respectively, and the orbital period is P =4.7464 days (Kiminki *et al.,* 2008). EY Cep is a double-lined eclipsing binary star and the components of EY Cep are young main-sequence stars with an age of about 40 million years. The spectral types are F0 + F0 V and the orbital period is P = 7.97143839 days (Sandberg Lacy *et al.,* 2006). HD 101131 is the brightest object in the young open cluster IC 2944. This system is a double-lined spectroscopic binary in an elliptical orbit with a period of P = 9.64659 days. It is a young system (approximately 2 million years old) and the spectral types are O6.5 V((f)) and O8.5 V for the primary and the secondary stars , respectively (Gies *et al.,* 2002). Haro 1-14c is a double-lined spectroscopic binary and consists of primary and secondary components. The spectral type is K3 and the orbital period is P = 591.3 days (Simon & Prato, 2004).

In the present paper we use a PNN to find optimum match to the four parameters from V_R curves of the four double-lined spectroscopic binary systems: Schulte 3, EY Cep, HD 101131, and Haro 1-14c. Our aim is to show the validity of our new method for a wide range of different types of binary systems.

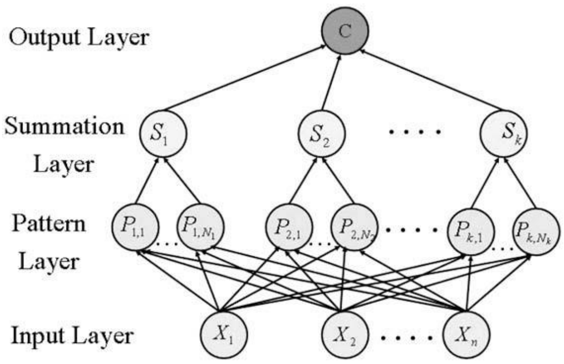

Figure 1. Schematic of a typical probabilistic neural network given by Bazarghan *et al.* (2008).

2. Materials and Methods

The radial velocity of a star in a binary system is defined as (Smart, 1990):

$$V_R = \gamma + \dot{Z} \tag{1}$$

where γ is the radial velocity of the center of mass of system with respect to the sun and

$$\dot{Z} = K[\cos(\theta + \omega) + e\cos\omega] \tag{2}$$

is the radial velocity of the star with reference to the center of mass of the binary (Smart, 1990). In Equation 2, the dot denotes the time derivative and θ, ω, and e are the angular polar coordinate (true anomaly), the longitude of periastron, and the eccentricity, respectively. Note that the quantities θ and ω are measured from the periastron point and the spectroscopic reference line (plane of sky), respectively.

Also,

$$K = \frac{2\pi}{P}\frac{a\sin i}{\sqrt{1-e^2}} \tag{3}$$

where P is the period of motion and inclination i is the angle between the line of sight and the normal of the orbital plane.

Here we apply the PNN method to estimate the four orbital parameters, *γ, K, e,* and ω of the V_R curve in Equation 2. The ANNs are able to acquire information and provide models even when the information and data are complex, noise contaminated, non-linear or incomplete. The goal of ANN is to map a set of input patterns onto a corresponding set of output patterns. The network accomplishes this mapping by learning from a series of past examples and defining the input and output sets for a given system. The network then applies what it has learned to a new input pattern to predict the appropriate output.

Previous papers applied methods with several stages for obtaining the four parameters *K*, *γ*, *ω*, and *e* from V_R. They obtained each of four parameters separately without dependence on numbers of V_R and ϕ. But by using the proposed PNN method, the number of stages decreased and four parameters have been calculated concurrently and, therefore, the speed of the calculations increased.

In this work, for the identification of the observational V_R curves, the input vector, X = (x_1, x_2, …, x_n), was the fitted V_R curve of a star with 36 data points (n = 36). The PNN is first trained to classify the V_R curves corresponding to all possible combinations of γ, *K*, *e*, and ω. This can synthetically generate V_R curves given by Equation 2 for each combination of parameters:

- $-100 \le \gamma \le 100$ in steps of 1;
- $1 \le K \le 300$ in steps of 1;
- $0 \le e \le 1$ in steps of 0.001;
- $0 \le \omega \le 360^\circ$ in steps of 5.

This gives a very large set of 5000 pattern groups *k*, where *k* denotes the number of different V_R classes, one class for each combination of γ, *K*, *e*, and ω. Since this very large number of different V_R classes causes some computational limitations, one can start with large step sizes. Note that from Petrie (1960), one can guess γ, *K*, and *e* from a V_R curve. This enables one to limit the range of parameters around their initial guesses. When the preliminary orbit has been derived after several stages, then one can use the above small step sizes to obtain the final orbit.

According to Equation 2 we obtained V_R for each combination of the parameters *K*, *γ*, *ω*, and *e* and different values of ϕ for $0 < \phi < 1$ (36 phase). Using the fitted curve to the observed data we obtained V_R from ϕ in these 36 phases. In this work, for the identification of the observational V_R curves, the input vector is the fitted V_R curve of a star. The PNN is first trained to classify V_R curves corresponding to all the possible combinations of *K*, *γ*, *ω*, and *e.* Since this is a very big number of different V_R classes with all the possible combinations of *K*, *γ*, *ω*, and *e*, we use the fitted V_R curve of a star. When an observational V_R curve of an unknown classification was fed to the trained network, we obtained four parameters with maximum similarity to all the possible combinations. Therefore this method is useful for all of the unknown parameters, For example, in one case, the method is useful for a star attended by two dark companions with commensurable periods.

When the network starts to train in big step sizes, its output is 1 for those inputs V_R and ϕ that have maximum similarity to combinations of the four parameters *K*, *γ*, *ω*, and *e*. For the other values of V_R, ϕ output is 0 and by repeating this process with a small step size it converges to the best values of *K*, *γ*, *ω*, and *e*. These combinations of the parameters give a very big set of *k* pattern groups, where *k* denotes the number of different V_R classes, one class for each combination of *K*, *γ*, *ω*, and *e*. Since this very big number of different V_R classe causes some computational limitations, one can first start with the big step sizes. Note that from Petrie (1960), one can guess *K*, *γ*, and *e* from a V_R curve. This enables one to limit the range of parameters around their initial guesses. When the preliminary orbit has been derived after several stages, then one can use the above small step sizes to obtain the final orbit. When the network starts to train with a determined step size, the maximum absolute error of the network's output and real value is smaller than the amount of mesh size and it outputs 1 for those inputs that have maximum similarity to four parameters. If we decrease the mesh size the error value between the real value and the network's output decreases.

The PNN has four layers including the input, pattern, summation, and output layers (Bazarghan *et al.*, 2008). When an input vector is presented, the pattern layer computes distances from the input vector to the training input vectors and produces a vector whose elements indicate how close the input is to a training input. The summation layer sums these contributions for each class of inputs to produce as its net output a vector of probabilities. Finally, a competitive transfer function on the output layer picks the maximum of these probabilities, and produces a 1 for that class and a 0 for the other classes (Specht, 1988, 1990). Thus, the PNN classifies the input vector into a specific k class labeled by the four parameters γ, *K*, *e*, and ω because that class has the maximum probability of being correct.

3. Results and Discussion

Using measured V_R data of the two components of these systems obtained by references in section 2, the fitted velocity curves are plotted in terms of the phase in Figures 2 through 5. We have fitted the observational V_R data by Curve Expert software. In this software, *r* is a parameter that quantifies goodness of fit. It is a fraction between 0.0 and 1.0, and has no units. Higher values indicate that the model fits the data better.

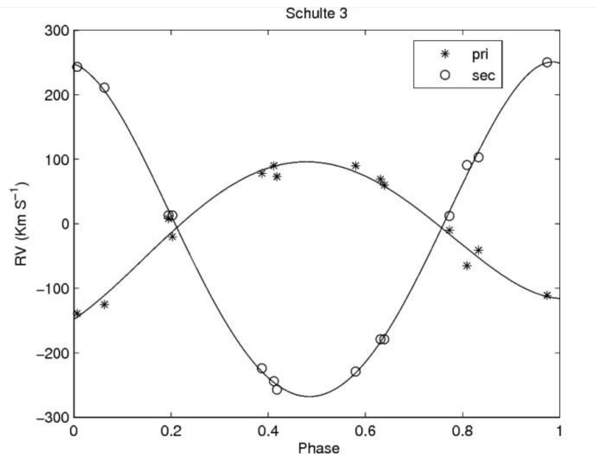

Figure 2. Radial velocities of the primary and secondary components of Schulte 3 plotted against the phase. The observational data have been measured by Kiminki *et al.* (2008).

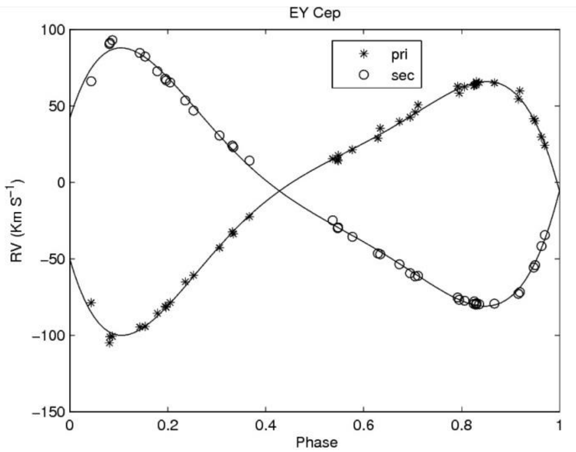

Figure 3. Radial velocities of the primary and secondary components of EY Cep plotted against the phase. The observational data have been measured by Sandberg Lacy *et al.* (2006).

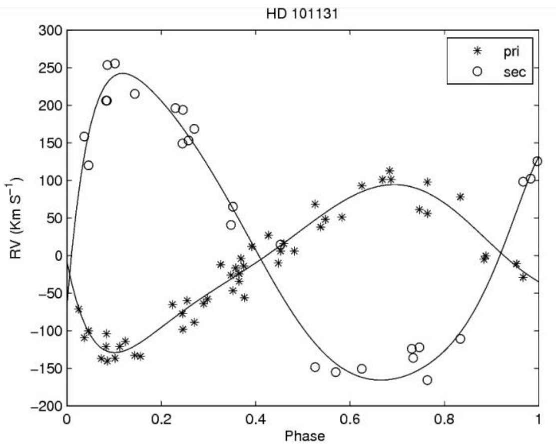

Figure 4. Radial velocities of the primary and secondary components of HD 101131 plotted against the phase. The observational data have been measured by Gies *et al.* (2002).

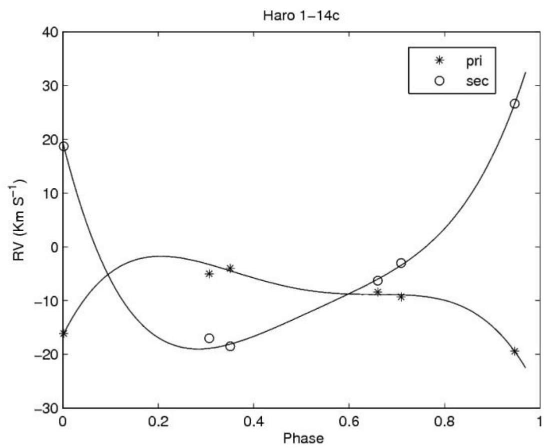

Figure 5. Radial velocities of the primary and secondary components of Haro 1-14c plotted against the phase. The observational data have been measured by Simon and Prato (2004).

The orbital parameters obtained from the PNN for Schulte 3, EY Cep, HD 101131, and Haro 1-14c are tabulated in Tables 1 through 4, respectively. The tables show that the results are in good accordance with those obtained by references in section 2. The numbers in parentheses in the last columns of the tables give the error in the last digit quoted. Note that the Gaussian errors of the orbital parameters in Tables 1 through 4 are produced by the same steps that generated the V_R curves, i.e. $\Delta\gamma = 1$, $\Delta K = 1$, $\Delta e = 0.001$, and $\Delta\varpi = 5$. When the network starts to train with the determined step size, the maximum absolute error of the networks output and real value is smaller than the amount of mesh size and it outputs 1 for those inputs that have maximum similarity to the four parameters. If we decrease the mesh size the error value between the real value and the network output decreases. The parameter *e* is the most important of the other three parameters that have been reported. The error of parameter *e* in this work is less than other methods. Furthermore the present method enables one to vary all of the unknown parameters γ, *K*, *e*, and ϖ simultaneously instead of one or two of them at a time. It is possible to make adjustments in the elements before the final result is obtained.

Table 1. Orbital parameters of Schulte 3.

	This Paper	Kiminki et al. (2008)
$\gamma\left(kms^{-1}\right)$	-26 ± 1	$-26.4(1.7)$
$K_p\left(kms^{-1}\right)$	113 ± 1	$113.2(14.5)$
$K_s\left(kms^{-1}\right)$	257 ± 1	$256.7(2.4)$
e	0.071 ± 0.001	$0.070(0.009)$
$\omega(^\circ)$	10 ± 5	$5.5(0.7)$

Table 2. Orbital parameters of EY Cep.

	This Paper	Sandberg Lacy et al. (2006)
$\gamma\left(kms^{-1}\right)$	-7 ± 1	-6.77 ± 0.10
$K_p\left(kms^{-1}\right)$	85 ± 1	85.23 ± 0.39
$K_s\left(kms^{-1}\right)$	87 ± 1	86.62 ± 0.14
e	0.441 ± 0.001	0.4415 ± 0.0012
$\omega(^\circ)$	110 ± 5	109.78 ± 0.07

Table 3. Orbital parameters of HD 101131.

	This Paper	Gies et al. (2002)
$\gamma_p\left(kms^{-1}\right)$	5 ± 1	-4.9 (25)
$\gamma_s\left(kms^{-1}\right)$	5 ± 1	11 (5)
$K_p\left(kms^{-1}\right)$	118 ± 1	117 (4)
$K_s\left(kms^{-1}\right)$	210 ± 1	211 (7)
e	0.155 ± 0.001	0.156 (29)
$\omega(^\circ)$	125 ± 5	122 (12)

Table 4. Orbital parameters of Haro 1-14c.

	This Paper	Simon & Prato (2004)
$\gamma\left(kms^{-1}\right)$	-9 ± 1	-8.71 ± 0.07
$K_p\left(kms^{-1}\right)$	8 ± 1	8.52 ± 0.13
$K_s\left(kms^{-1}\right)$	27 ± 1	27.5 ± 1.3
e	0.616 ± 0.001	0.617 ± 0.008
$\omega(^\circ)$	230 ± 5	232.90 ± 0.55

These are close to the observational errors reported in the literature. Regarding the estimated errors, following Specht (1990), the error of the decision boundaries depends on the accuracy with which the underlying probability density functions (PDFs) are estimated. Parzen (1962) proved that the expected error gets smaller as the estimate is calculated from a progressively larger data set. This definition of consistency is particularly important since it means that the true distribution will be approached in a smooth manner. Specht (1990) showed that a very large value of the smoothing parameter would cause the estimated errors to be Gaussian regardless of the true underlying distribution. Also, the misclassification rate is stable and does not change dramatically with small changes in the smoothing parameter.

The combined spectroscopic elements including $m_p \sin^3 i$, $m_s \sin^3 i$, $(m_p + m_s)\sin^3 i$, $(a_p + a_s)\sin i$, and $\frac{m_s}{m_p}$ are calculated by substituting the estimated parameters *K*, *e*, and ω into Equations 3, 15, and 16 in Karami and Teimoorinia (2007). The results obtained for the four systems are tabulated in Tables 5 through 8 and show that our results are in good agreement with those obtained by references in section 2. Here the errors of the combined spectroscopic elements in Tables 5 through 8 are obtained by the help of errors in orbital parameters error, such as Equations 3, 15, and 16 in Karami and Teimoorinia (2007).

Table 5. Combined spectroscopic elements of Schulte 3.

Parameter	This Paper	Kiminki et al. (2008)
$m_p \sin^3 i/M_\odot$	17.1710 ± 0.2561	$17.2(0.3)$
$m_s \sin^3 i/M_\odot$	7.5499 ± 0.1501	$7.6(1.4)$
$(m_p + m_s)\sin^3 i/M_\odot$	24.7209 ± 0.4062	—
$a_p \sin i/R_\odot$	7.3566 ± 0.0656	$7.4(0.9)$
$a_s \sin i/R_\odot$	16.7315 ± 0.0663	$16.7(0.2)$
$(a_p + a_s)\sin i/R_\odot$	24.0881 ± 0.1319	$24(0.9)$
m_s/m_p	0.4397 ± 0.0057	$0.44(0.08)$

PNNs are used in both regression (including parameter estimation) and classification problems (Agarwal *et al.*, 2012; Almeida *et al.*, 2010; Andreon *et al.*, 2000; Ball *et al.*, 2004; Cortiglioni *et al.*, 2001; Firth *et al.*, 2003; Snider *et al.*, 2001). However, one can discretize a continuous regression problem to such a degree that it can be represented as a classification problem (Specht, 1988, 1990), as we did in this work.

There are different methods to determine the orbit of a spectroscopic binary from its V_R curve. Using the measured V_R data of Schulte 3, EY Cep, HD 101131, and Haro 1-14c obtained by other methods in the literature, we find the orbital elements of these systems by the PNN. Our results show that this method has more advantages in comparison with the other traditional methods.

4. Conclusions

We showed the validity of this method to a wide range of different types of binary systems. Our numerical results are in good agreement with those obtained by others using more traditional methods. In this method the time consumed is considerably less than in the other methods and it is applicable to orbits of all eccentricities and inclination angles. It is also more accurate as the orbital elements are deduced from all points of the velocity curve instead of four in the method of Lehmann-Filhés. The present method enables one to vary all of the unknown parameters γ , K, e, and ω simultaneously instead of one or two of them at a time. It is possible to make adjustments in the elements before the final result is obtained. There are some cases, for which the geometrical methods are inapplicable, and in these cases the present one may be found useful. Another case, for which this method is useful, is that of a star attended by two dark companions with commensurable periods.

Acknowledgments

This work has been supported financially by Islamic Azad University, Marivan Branch, Marivan, Iran.

References

Agarwal, S., Abdalla, F. B., Feldman, H. A., Lahav, O., & Thomas, S. A. (2012). PkANN–I. Non-linear matter power spectrum interpolation through artificial neural networks. *Monthly Notices of the Royal Astronomical Society, 242*, 1409–1418.

Almeida, C., Baugh, C. M., Lacey, C. G., Frenk, C. S., Granato, G. L., Silva, L., & Bressan, A. (2010). Modelling the dusty universe–I. Introducing the artificial neural network and first applications to luminosity and colour distributions. *Monthly Notices of the Royal Astronomical Society, 402*, 544–564.

Andreon, S., Gargiulo, G., Longo, G., Tagliaferri, R., & Capuano, N. (2000). Wide Field Imaging. I. Applications of Neural Networks to object detection and star/galaxy classification. *Monthly Notices of the Royal Astronomical Society, 319*, 700-716.

Ball, N. M., Loveday, J., & Fukugita, M. (2004). X Galaxy types in the Sloan Digital Sky Survey using supervised artificial neural networks. *Monthly Notices of the Royal Astronomical Society, 348*, 1038-1046.

Bazarghan, M., Safari, H., Innes, D. E., Karami, E., & Solanki, S. K. (2008). A nanoflare model for active region radiance: application of artificial neural networks. *Astronomy and Astrophysics, 492*, L13-L16.

Cortiglioni, F., Mahonen, P., Hakala, P., & Frantti, T. (2001). Automated Star-Galaxy Discrimination for Large Surveys. *The Astrophysical Journal, 556*, 937-943.

Firth, A. E., Lahav, O., & Somerville, R. S. (2003). Estimating photometric redshifts with artificial neural networks. *Automated Star-Galaxy Discrimination for Large Surveys, 339*, 1195-1202.

Gies, D. R., Penny, L. R., Mayer, P., Drechsel, H., & Lorenz, R. (2002). Tomographic Separation of Composite Spectra. X. The Massive Close Binary HD 101131. *The Astrophysical Journal, 574*, 957-962.

Karami, K., & Teimoorinia, H. (2007). Velocity curve analysis of the spectroscopic binary stars by the non-linear least squares. *Astrophysics and Space Science, 311*, 435-442.

Karami, K., & Mohebi, R. (2007a). Velocity Curve Analysis of Spectroscopic Binary Stars AI Phe, GM Dra, HD 93917 and V502 Oph by Nonlinear Regression. *Chinese Journal of Astronomy and Astrophysics, 7*, 558-564.

Karami, K., & Mohebi, R. (2007b). Velocity curve analysis of the spectroscopic binary stars PV Pup, HD 141929, EE Cet and V921 Her by nonlinear regression. *Journal of Astrophysics and Astronomy, 28*, 217-230.

Karami, K., & Mohebi, R. (2009). Velocity curve studies of spectroscopic binary stars V380 Cygni, V401 Cyg, V523 Cas,V373 Cas and V2388 Oph. *Journal of Astrophysics and Astronomy, 30*, 153-163.

Karami, K., Mohebi, R., & Soltanzadeh, M. M. (2008). Application of a new non-linear least squares velocity curve analysis technique for spectroscopic binary stars. *Astrophysics and Space Science, 318*, 69-71.

Kiminki, D. C., McSwain, M. V., & Kobulnicky, H. A. (2008). New Massive Binaries in the Cygnus OB2 Association. *The Astrophysical Journal, 679*, 1478-1489.

Lehmann-Filhés, R. (1894). Ueber die Bestimmung einer Doppelsternbahn aus spectroskopischen Messungen der im Visionsradius liegenden Geschwindigkeitscomponente. *Astronomische Nachrichten, 136*, 17-30.

Parzen, E. (1962). On Estimation of a Probability Density Function and Mode. *Annals of Mathematical Statistics, 33*, 1065-1076.

Petrie, R. M. (1960). *Astronomical Techniques*. Chicago, IL: University of Chicago Press.

Russell, H. N. (1902). An Improved Method of Calculating the Orbit of a Spectroscopic Binary. *Astrophysical Journal, 15*, 252-260.

Sandberg Lacy, C. H., Torres, G., Claret, A., & Menke, J. L. (2006). Absolute Properties of the Main-Sequence Eclipsing Binary Star EY Cephei. *The Astronomical Journal, 131*, 2664-2672.

Simon, M., & Prato, L. (2004). The Double-lined Spectroscopic Binary Haro 1-14c. *The Astrophysical Journal, 613*, L69-L71.

Smart, W. M. (1990). *Textbook on Spherical Astronomy* (6^{th} ed.). Cambridge, England: Cambridge University Press.

Snider, S., Prieto, C. A., von Hippel, T., Beers, T. C., Sneden, C., Qu, Y., & Rossi, S. (2001). Three-dimensional spectral classification of low-metallicity stars using Artificial Neural Networks. *The Astrophysical Journal, 562*, 528-548.

Specht, D. F. (1988). Probabilistic neural networks for classification, mapping, or associative memory. *Proceedings of the IEEE International Conference on Neural Networks 1*, 525-532.

Specht, D. F. (1990). Probabilistic neural networks. *Neural Networks, 3*, 109-118.

Sterne, T. E. (1941). Notes on Binary Stars. V. The Determination by Least-Squares of the Elements of Spectroscopic Binaries. *Proceedings of the National Academy of Sciences of the United States of America 27,* 175-181.